Effect of Styrene-*co*-Acrylonitrile on Cold Crystallization and Mechanical Properties of Poly(ethylene terephthalate)

Renate M. R. Wellen,[1] Eduardo L. Canedo,[2] Marcelo S. Rabello[3]

[1]*Department of Chemical Engineering, Federal University of Pernambuco, PE, Brazil*
[2]*PolyTech, Prospect, Connecticut*
[3]*Department of Materials Engineering, Federal University of Campina Grande, PB, Brazil*

Received 4 February 2011; accepted 27 November 2011
DOI 10.1002/app.36585
Published online 30 January 2012 in Wiley Online Library (wileyonlinelibrary.com).

ABSTRACT: Blends of poly(ethylene terephthalate) (PET) with small amounts of styrene-*co*-acrylonitrile (SAN) were prepared by melt blending, and cold crystallization of these mixtures was investigated by means of differential scanning calorimetry. The results suggest that SAN interacts with the amorphous phase of PET, as observed by variations in the glass transition temperature and in the morphology of the blends, analyzed by scanning electron microscopy. The addition of 1% SAN promoted a significant reduction in the crystallization rate of PET, in a manner similar to that of an antinucleating agent. However, the crystallinity of the PET/SAN blends was comparable with that of neat PET; hence, mechanical properties were only slightly affected. Kinetic parameters were determined using Avrami theory; Avrami plots presented a nonlinear behavior at the end of crystallization, indicating that cold crystallization proceeds in two stages. © 2012 Wiley Periodicals, Inc. J Appl Polym Sci 125: 2701–2710, 2012

Key words: cold crystallization; blends; PET; SAN

INTRODUCTION

Polymer blends is a promising field in polymer science and engineering and have attracted much attention in both the academic and industrial communities. The possibility of developing new materials with better properties in little time and with minimum investment is the driving force for this interest. The crystallization behavior of polymers and polymer blends is relevant to the potential use of these materials in demanding engineering applications. The field continues to attract considerable interest as it involves important issues concerning control of super molecular structure and its effect on material properties.[1–3]

Poly(ethylene terephthalate) (PET) is a semicrystalline thermoplastic polyester with interesting thermal and mechanical properties, good chemical resistance, low permeability to gases, and excellent processability. PET and PET blends have many applications in packaging, fibers, electrical equipments, automotive and construction industries, etc. Although the properties of PET are controlled mainly by its chemical structure, the crystallinity and morphology also play a major role. Thus, the study of how the structure of PET is affected by crystallization conditions may be highly relevant to obtain products with desirable properties. Moreover, the crystallization of PET with industrial processing techniques, such as blow molding and thermoforming, occur normally in a two-stage process. First, an amorphous preform (for the case of blow molding) is obtained by injection molding in a cold mold. Then, this preform is heated above the glass transition temperature and is finally stretched and blown to the final shape. If partial crystallization occurs during the preform production or during the heating stage before blowing, the product may be unsuitable for bottle production. Actually, this is one of the major concerns of industry. The ideal situation, therefore, occurs when cold crystallization is delayed and the final mechanical and physical properties are achieved. One way to reach this goal, adding small amounts of an amorphous polymer to PET, was studied by the authors in previous work. Both polystyrene and styrene-*co*-acrylonitrile (SAN) were shown to act as "antinucleating" agents, lowering the rate of cold crystallization of PET without changing the transparency of the material under processing conditions.[4,5]

In this work, the effect of small amounts of amorphous SAN on the isothermal cold crystallization of PET is studied by differential scanning calorimetry (DSC). Kinetic parameters were determined according to Avrami[6–8] theory, and the activation energy for crystallization was established using Arrhenius

Correspondence to: M. S. Rabello (marcelo@dema.ufcg.edu.br).
Contract grant sponsor: FACEPE (Brazil).

TABLE I
Thermal Transition Temperatures of PET and SAN[10]

Polymer	T_g (°C)	T_c (°C)	T_m (°C)
PET	70	124	250
SAN	107	–	–

plots. The equilibrium melting temperature was determined following Hoffman and Weeks.[9] The morphology of PET/SAN blends was analyzed by scanning electron microscopy (SEM), and mechanical properties were determined in amorphous and semicrystalline samples.

The isothermal cold crystallization of PET/polystyrene (PS) blends[4] and the nonisothermal crystallization of PET/SAN[5] was reported previously.

EXPERIMENTAL

Materials

Bottle grade PET (Rhopet S78), with intrinsic viscosity 0.78 dL/g and weight-average molar mass of 48 kg/mol was supplied by Rhodia-Ster (São Paulo, Brazil) (Rhopet S78). Injection molding grade SAN (Luran 358N) was purchased from BASF (São Paulo, Brazil). Thermal transition temperatures of the materials are presented in Table I.

Processing

Before processing, PET was dried at 120°C during 6 h to avoid the hydrolysis,[11,12] and SAN was dried at 80°C during 14 h to remove moisture.[11,13,14] Most of this work is based on the study of blend of 99% PET and 1% SAN (percentages by weight) and its comparison with neat PET resin, but a PET/SAN blend with 15% SAN was also prepared and used for showing the phase morphology (Fig. 11).

Blends were prepared by two procedures: batch mixing and continuous extrusion compounding. Samples of neat PET were processed in the same way, to compare results on materials with the same processing history.

For thermal analysis, samples were obtained by melt mixing in a laboratory internal mixer Haake Rheomix 600 (Waltham, MA, USA) fitted with high intensity rotors ("roller" type), operating at 265°C and 60 rpm for 10 min. After compounding, the molten material was quenched in a water/ice bath to obtain an amorphous blend.

To evaluate the mechanical properties, PET and the blends were compounded in a conical counter-rotating twin-screw extruder Haake TW100, operating at 260°C and 60 rpm. Pelletized material was dried and then injection molded in a chilled mold (~ 10°C) to obtain amorphous test specimens, according ASTM D-638. Some of these specimens were heated to cold crystallize, and the mechanical properties of amorphous and semicrystalline materials were compared.

To verify the absence of crystallinity in the "amorphous" injected specimens, bars of PET and PET/SAN blends were submitted to the X-ray diffraction analysis. Typical diffractograms, presented in Figure 1, show the wide band characteristic of amorphous polymers.[15]

DSC

The melting and crystallization behavior of PET and the PET/SAN blend were determined using a Shimadzu (Kyoto, Japan) DSC-50 equipment, calibrated from the enthalpy of fusion of a known mass of ultra-pure indium.

Isothermal cold crystallization conditions were achieved by quick heating (~ 100°C/min) the samples from room temperature to the target crystallization temperature, ranging from 110°C to 160°C. If crystallization started before the target temperature was reached, the measurement was discarded. The DSC output (mW) was registered as a function of time, as long as no change from the baseline was observed. For each experimental condition, at least three scans were made. From these tests, the melting temperature T_m (°C), latent heat of crystallization per unit mass ΔH_c (kJ/kg), and latent heat of melting per unit mass ΔH_m (kJ/kg) were determined. Latent heats measured in blends were normalized dividing by the mass fraction of crystallizable polymer (PET) in the blend. Mass based crystallinity X was obtained from:

$$X = \frac{\Delta H_m}{\Delta H_m^0} \tag{1}$$

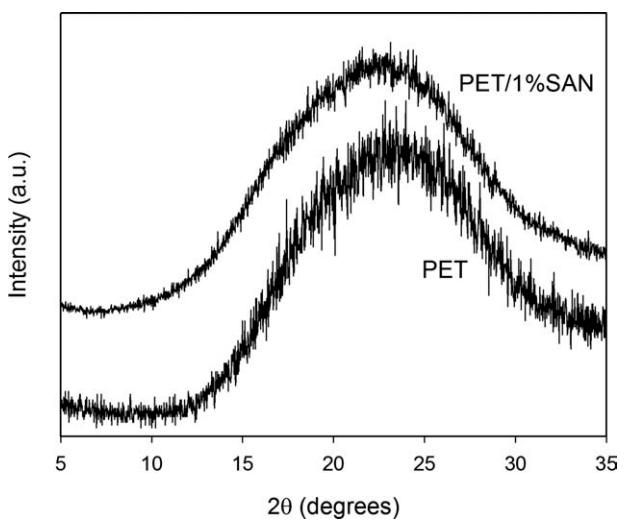

Figure 1 X-ray diffractograms of PET and a PET/SAN blend with 1% SAN.

where ΔH_m^0 is the latent heat of melting for the pure crystalline phase, taken as 117.65 kJ/kg.[16,17]

The effect of isothermal crystallization temperature on the melting behavior of PET and its blends was analyzed by heating the cold crystallized samples at 10°C/min to complete melting (at about 270°C). The equilibrium melting temperature (T_m^0) was determined according to Hoffman and Weeks.[9] The kinetics of isothermal cold crystallization was studied using Avrami's approach.[8]

Nonisothermal cold crystallization tests were performed by heating the glassy samples from room temperature to 300°C at heating rates ranging from 1°C/min to 50°C/min. The effect of heating rate on the glass transition temperature of the blend was determined.

SEM

A Shimadzu SSX 550 Superscan SEM was used to study the phase morphology of PET/SAN blends. Injected test specimens were cryogenically fractured in liquid nitrogen, and the fractured surface was covered with gold to avoid the accumulation of charges.[18] A minimum of four photographs were taken for each sample, and about 200 particles were considered to determine the number-average domain diameter (d_m) of the disperse phase according to:[19]

$$d_m = \frac{\sum n_i d_i}{n} \quad (2)$$

where n_i is the number of particles of diameter d_i, and n is the total number of particles.

Mechanical properties

Tensile tests according to ASTM D-638 were performed using a Lloyd Instruments model LR10K (West Sussex, UK) universal testing machine. The tests on PET and the PET/SAN blend, both amorphous and cold crystallized, were conducted at 23°C, at a crosshead speed of 5 mm/min; the average of six runs of each formulation was reported.

RESULTS AND DISCUSSION

Glass transition temperature

Figure 2 shows the effect of heating rate on glass transition temperature (T_g) of PET and the PET/SAN blend with 1% SAN. In both cases, T_g increases with the heating rate, which may result from the time lag for molecular relaxation in the glass transition region. The PET/SAN blend shows a higher transition temperature than the neat PET at all heating rates, up to about 7.5°C at heating rates above 30°C/min. This trend may be associated, in part, with the higher T_g of SAN (Table I). Although PET/SAN blends are immiscible,[5,20] the behavior shown in Figure 2 for such a low level of SAN suggests also the effect of specific intermolecular interactions.[21,22] This may have influenced the crystallization behavior of PET/SAN blends, as discussed below.

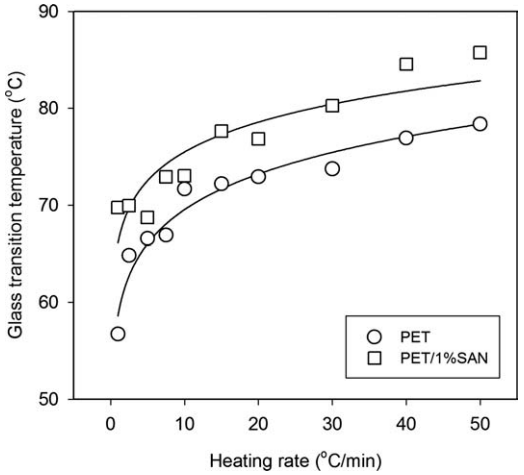

Figure 2 Effect of heating rate on the glass transition temperature (T_g) of PET and a PET/SAN blend with 1% SAN.

Isothermal cold crystallization

Figure 3 shows DSC exotherms for the isothermal cold crystallization of PET and the PET/SAN blend with 1% SAN at different temperatures. The effect of temperature on the cold crystallization behavior is well known and has been previously observed in PET[23–25] and PET copolymers:[26] crystallization peaks become sharper and crystallization rates increase with increasing temperature, probably as a result the lower viscosity and increase in molecular mobility, which facilitates crystalline ordering.[27,28]

At the same crystallization temperature, the presence of SAN increased the crystallization time and broadened the crystallization peak, evidencing a decrease in the crystallization rate of PET. The reduction in crystallization rate may be related to the amorphous character of SAN as well as to its polar nature, which may hinder macromolecular mobility.

The blend with 1% SAN was selected for this study because it was observed elsewhere[10] that an increase of the SAN fraction to 10% to 20% on the PET/SAN blends does not have a significant additional impact on the reduction of the crystallization rate of PET. Similar behavior was previously verified for PET/PS blends.[4,29]

The evolution of relative crystallinity x with time was computed from the DSC exotherms and are

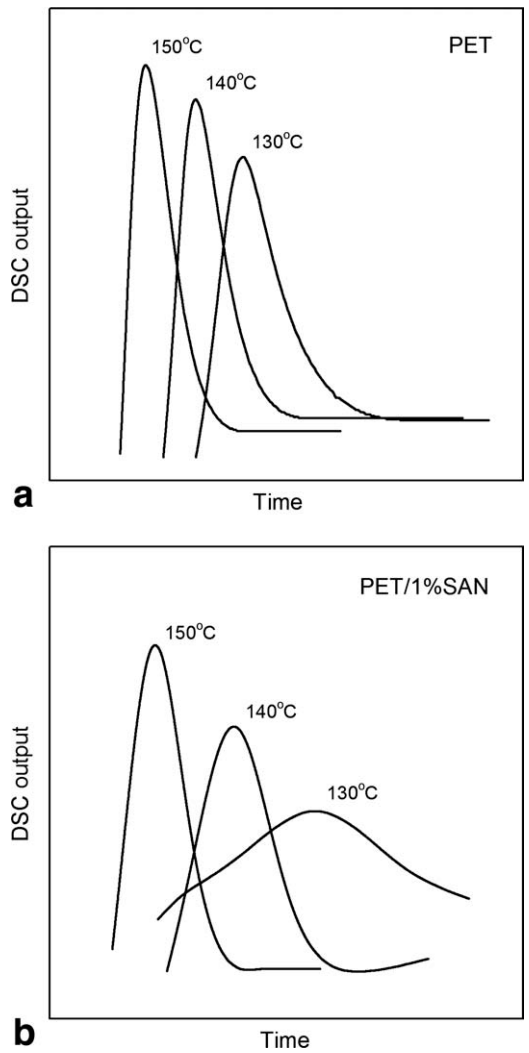

Figure 3 DSC exotherms for isothermal cold crystallization of PET (a) and a PET/SAN blend with 1% SAN (b).

plotted in Figure 4. All isotherms are sigmoidal in shape, characteristic of phase transformations without discontinuities, which is typical of polymers.[10] The curves are superimposable by a shift of the time axis, revealing that the solidification process of PET and the PET/SAN blend, while marked by differences in nucleation and crystalline growth rates, does not differ greatly in growth morphology.[30–33]

As an example, Figure 5 compares the crystallization isotherms of PET and the PET/SAN at 130°C. The delay in PET crystallization caused by the presence of only 1% of noncrystallizable SAN is remarkable. When crystallization in neat PET reaches the end, only 45% of PET has crystallized in the blend.

The macroscopic rate of crystallization, $c = dx/dt$ obtained from the $x = x(t)$ plots of Figure 5 is an important characteristic of the crystallization process. Although c varies with the relative crystallinity, average values are useful parameters. In general, we define:

$$\bar{c}_{x_1-x_2} = \frac{x_2 - x_1}{\Delta t_{12}} \tag{3}$$

where Δt_{12} is time required to change the relative crystallinity from x_1 to x_2. In this work, we use the average rate of crystallization between 20% and 80% relative crystallinity as a representative value of the overall rate of crystallization.

Figure 6(a) shows the effect of crystallization temperature on $\bar{c}_{0.2-0.8}$ for PET and a PET/SAN blend with 1% SAN. The rate of cold crystallization increases significantly with the crystallization temperature; $\bar{c}_{0.2-0.8}$ increases 3.5 times for a 40°C rise in temperature for neat PET and 5.5 times for the same temperature rise in the PET/SAN blend. Moreover, the presence of 1% SAN lowers the crystallization rate of PET in 20%–60% at the temperature range analyzed.

The rate of crystallization is frequently characterized in the technical literature[32,34,35] by the crystallization

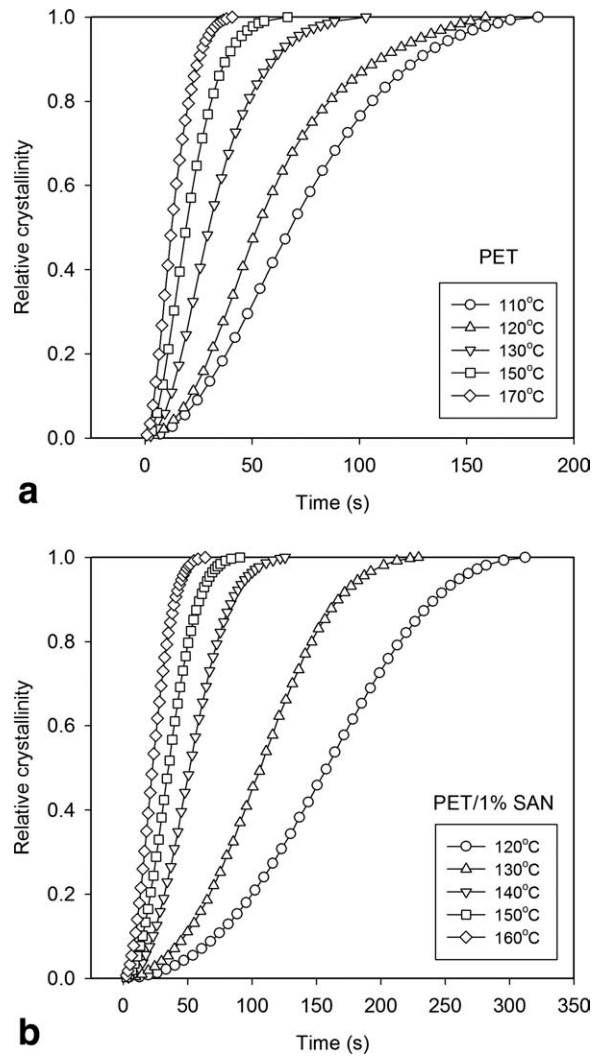

Figure 4 Evolution of relative crystallinity with time during the isothermal cold crystallization of PET (a), and of a PET/SAN blend with 1% SAN (b), at different temperatures. Notice the different time scale.

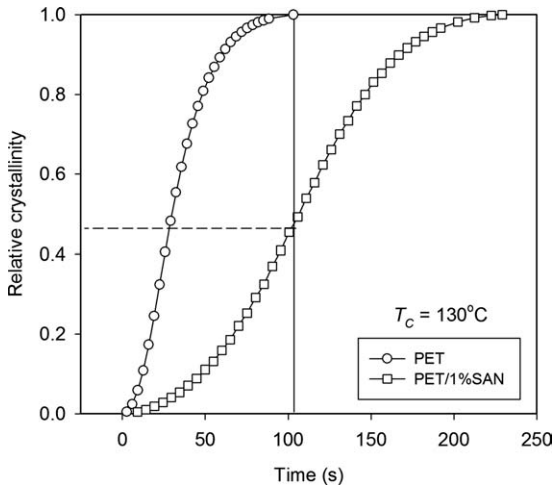

Figure 5 Evolution of relative crystallinity with time during the isothermal cold crystallization of PET and a PET/SAN blend with 1% SAN at 130°C.

half-time, $t_{0.5}$, the time needed to reach 50% relative crystallinity from the starting point of the process. The reciprocal of the crystallization half-time, $1/t_{0.5}$, is often presented as a measure of the rate of crystallization.[34] In fact, $1/t_{0.5}$, is proportional to the average crystallization time between the starting ($x = 0$) and mid-point ($x = 0.5$) of crystallization ($\bar{c}_{0-0.5}$ in our notation). As expected, $t_{0.5}$ increases with temperature for both the neat PET and the PET/SAN blend. The presence of 1% SAN increases the crystallization half-time 80% to 200% depending on temperature. Figure 6(b) shows the effect of temperature on the crystallization half-time for PET and a PET/SAN blend with 1% SAN.

The decrease of the crystallization rate of PET on addition of 1% of noncrystallizable component (SAN) may be related to several factors, such as an increase of the melt viscosity,[36,37] to molecular segregation of the second component,[38,39] to the limited solubility among components,[2,40,41] to an increase of the activation energy for the isothermal crystallization,[42] and—in general—to a decrease of the "crystallizability" of PET.[43]

During the crystallization process, crystallizable material is continually driven toward the growing crystal, while the noncrystallizable components (atactic and low-molecular mass chains) is rejected away or accumulated within the crystalline phase. According to Keith and Padden,[38,39] the place where the noncrystallizable material segregates (the distance δ from the crystal font) depends on the interplay between crystal growth and diffusion, governed by the dimensional parameter:

$$\lambda = \frac{G\delta}{D} \tag{4}$$

where G is the linear rate of advance of the crystal front and D is the diffusivity of the noncrystallizable material. For fast crystal growth ($\lambda >> 1$), diffusion cannot cope and impurities accumulate between the lamellae. On the other hand, for slow crystal growth ($\lambda << 1$), diffusion carries impurities away from crystal, which end up accumulating in the interfibrillar or interspherulitic regions. In any case, the presence of impurities hinders the crystallization process.

The chemical structure of PET chains, alternating flexible aliphatic groups and stiff aromatic ones, favors a relatively slow rate of crystallization. The slowing down of the crystallization in the PET/SAN blend suggests that the noncrystallizable amorphous SAN chains are located away from the lamellae, between the fibrils or spherulites.

Fillers,[44,45] polymers,[46,47] and copolymers[48,49] are added to PET to modify its crystallization behavior. Additives may be used to facilitate (nucleating agents)[50–52] or to hinder (antinucleating agents)[26,53,54] the crystallization of PET. Additives that modify the

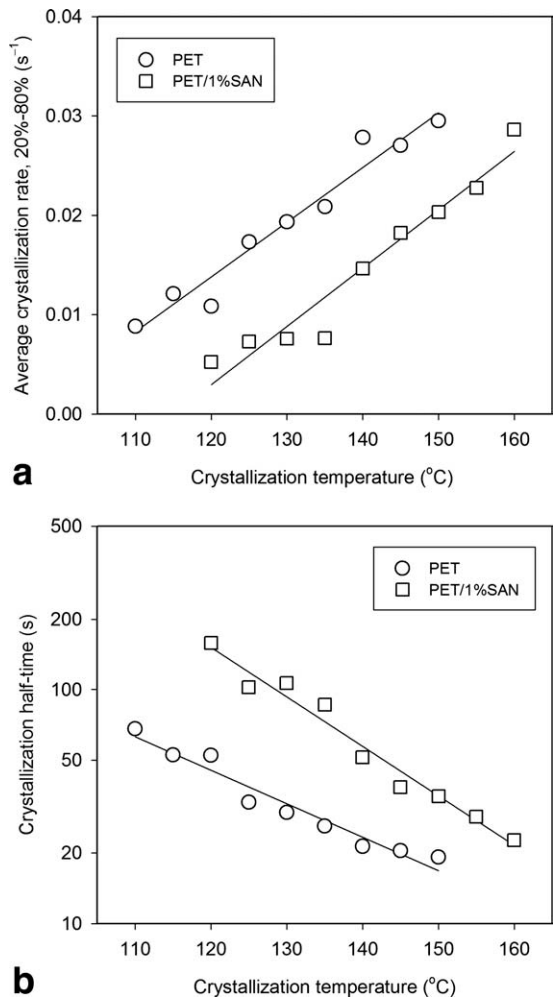

Figure 6 Effect of the temperature on the average crystallization rate $c_{0.2-0.8}$ (a) and on the crystallization half-time $t_{0.5}$ (b) of PET and a PET/SAN blend with 1% SAN.

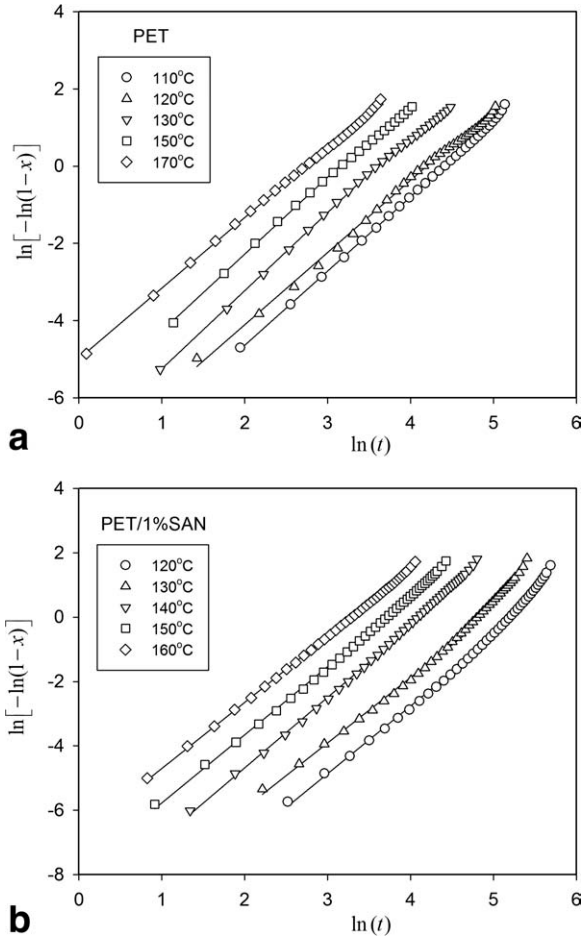

Figure 7 Avrami plots for the isothermal cold crystallization of PET (a) and a PET/SAN blend with 1% SAN (b).

crystallization characteristics without adversely affecting other properties are particularly valuable. Those that interfere with the development of crystallinity may be of application in areas where product transparency is important (such as PET bottles). SAN seems to be this kind of "ideal" additive: it significantly delays crystallization of PET when added in amounts small enough to preserve the mechanical properties that make PET so desirable (see Table V).

Kinetics of isothermal cold crystallization—Avrami model

Avrami[6–8] modeled the isothermal crystallization process as:

$$x = 1 - \exp(-Kt^n) \tag{5}$$

where x is the fractional crystallinity at time t, n is the Avrami exponent, which depends on the nature of the nucleation and growth geometry and mechanism, and K is a temperature-dependent rate constant. Equation (5) may be written as:

$$\ln[-\ln(1-x)] = \ln\ K + n\ \ln\ t \tag{6}$$

The Avrami parameters n and K may be obtained from the slope and intercept in a plot of $\ln[-\ln(1-x)]$ versus $\ln t$ as shown in Figure 8 for the cold crystallization data of PET and the PET/SAN blend.

Avrami plots show evidence that the cold crystallization developed in two stages: a first, clearly linear, primary crystallization phase, followed by a nonlinear secondary crystallization phase, more evident in the PET/SAN blend [Fig. 7(b)]. Secondary crystallization[55,56] has been observed in different polymer systems, such PET,[57] polyethylene (PE),[27] polypropylene (PP),[58] poly(p-phenylene sulfide) ou poly(phenylene sulfide) (PPS),[59] blend of poly(ethylene oxide) and poly(ether sulfone) (PEO/PES),[60] poly(ether ether ketone) (PEEK),[61] and PET/poly(ether imide) (PEI).[62] For blends with noncrystallizable components, the second stage in Avrami plots may be related to molecular segregation of the second component contributing to a decrease crystalline growth rate. Similar behavior has been observed in blends like PEO/PES,[60] blend of linear polyethylene with low density polyethylene (LPE/LDPE),[63] sPS/iPS, and sPS/aPS.[64]

The parameters n_1 and K_1 were determined for the primary crystallization stage; approximate linearized parameters n_2 and K_2 were estimated for the secondary crystallization stage. Results are shown in Table II and Figure 8.

TABLE II
Avrami Parameters for the First (n_1, K_1) and Second (n_2, K_2) Stages of the Isothermal Cold Crystallization of PET and a PET/SAN Blend with 1% SAN

	PET				PET/1%SAN			
T_c (°C)	n_1	ln K_1	n_2	ln K_2	n_1	ln K_1	n_2	ln K_2
110	1.93	−8.497	2.33	−10.448	–	–	–	–
120	1.88	−7.875	2.10	−9.028	2.11	−11.176	2.10	−11.176
130	2.00	−7.220	1.74	−6.309	2.06	−10.102	2.78	−13.816
140	1.98	−6.490	–	–	2.24	−9.200	2.47	−10.152
150	1.90	−6.068	–	–	2.14	−7.949	2.61	−9.864
160	–	–	–	–	2.05	−6.752	–	–

K_1 and K_2 in s^{-n}.

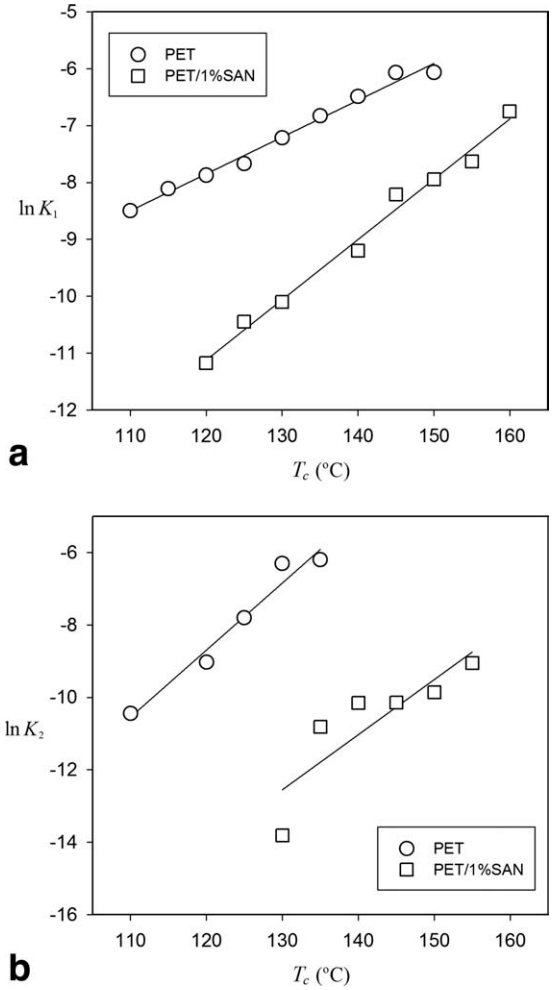

Figure 8 Effect of temperature on K_1 (a) and K_2 (b) rate constants for PET and the PET/SAN blend with 1% SAN.

For the first stage, the Avrami exponent n is close to 2 for both PET and the blend with 1% SAN, consistent with two-dimensional, diffusion-controlled crystal generated by heterogeneous nucleation.[6–8] Similar values of n were previously obtained for PET[45,47,51] and for blends with PET.[65] The rate constant K increased with temperature, probably as a consequence of higher molecular mobility and is significantly lower for the blend than for the neat PET, due to the reduction of the crystallization rate by the presence of a noncrystallizable component. These results are consistent with those shown in Figure 7.

Activation energy

The rate of crystallization is obtained differentiating eq. (5):

$$c = \frac{dx}{dt} = nKt^{n-1}(1-x) \tag{7}$$

Eliminating the time between eqs. (5) and (7):

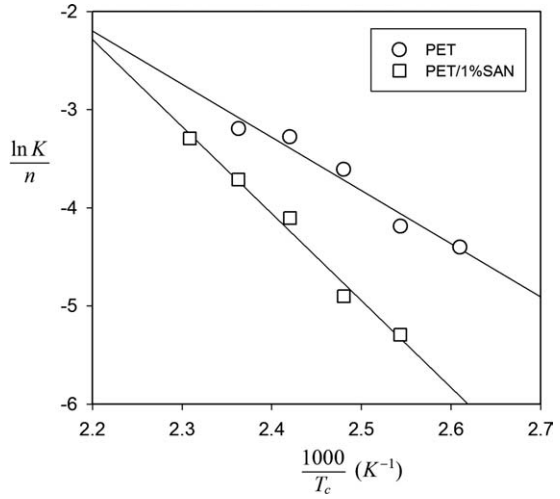

Figure 9 Arrhenius plot for the activation energy for the first stage of isothermal cold crystallization of PET and a PET/SAN blend with 1% SAN.

$$c = nK^{1/n}(1-x)[-\ln(1-x)]^{1-1/n} \tag{8}$$

Assuming that Avrami exponent n is independent of temperature, which is borne (approximately) by the experimental data, especially for the first stage, eq. (8) shows that $k = K^{1/n}$ is a proper kinetic "constant" for the thermally activated crystallization process.[66,67] The kinetic constant can be expressed in terms of an activation energy ΔE:

$$K^{1/n} = k_0 \exp\left(\frac{\Delta E}{RT}\right) \tag{9}$$

where k_0 is a pre-exponential factor independent of temperature and $R = 8314$ J/mol·K is the universal gas constant. ΔE for the first crystallization stage was obtained by linear regression of $\ln K_1^{1/n1}$ vs. $1/T_c$ (Fig. 9). Results are shown in Table III, along with the mean value of the Avrami exponent.

The higher value of the activation energy obtained for the blend indicates that cold crystallization is thermically less favored by the presence of a noncrystallizable "impurity," in accordance with results shown throughout this article.

Introducing eq. (9) into eq. (8), we obtain an expression of the rate crystallization in terms of the

TABLE III
Pre-Exponential Factor, Activation Energy and Mean Avrami Exponent for the First Stage of Isothermal Cold Crystallization of PET and a Blend with 1% SAN

Material	ln k_0	ΔE (kJ/mol)	$\overline{n_1}$
PET	9.711	45.0	1.94 ± 0.06
PET/1%SAN	17.200	73.6	2.12 ± 0.09

k_0 in s^{-1}.

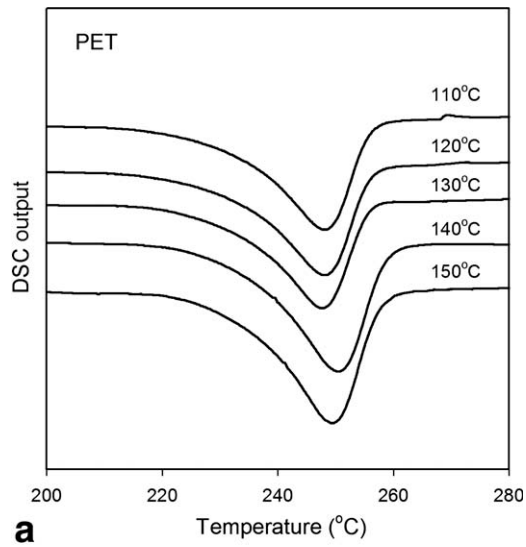

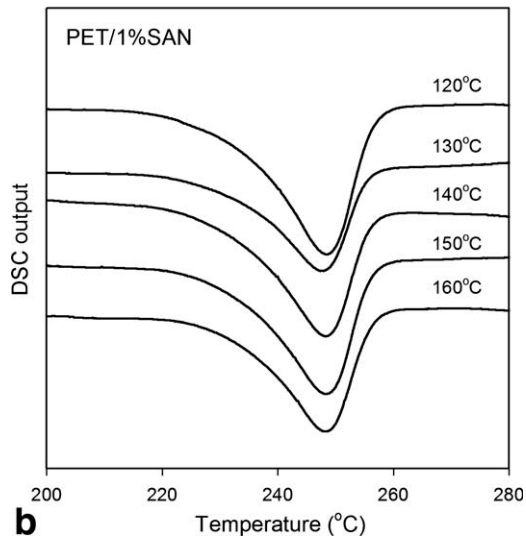

Figure 10 Melting endotherms of PET (a) and PET/SAN blend (b); isothermal cold crystallization temperatures indicated.

relative crystallinity x, temperature T, and temperature-independent constants (n, k_0, ΔE) that is particularly useful for process modeling and simulation:

$$c = nk_0 \exp(-\Delta E/RT) \cdot (1-x)[-\ln(1-x)]^{1-1/n} \quad (10)$$

TABLE IV
Equilibrium Melting Temperature (T_m^0), Latent Heat of Fusion (ΔH_m), and Mass Crystallinity (X) of PET and its Blend with 1% SAN

Composition	PET	PET/SAN (1%)
T_m^0 (°C)	255	248
ΔH_m (kJ/kg)	31.0	28.6
X (%)	26	25

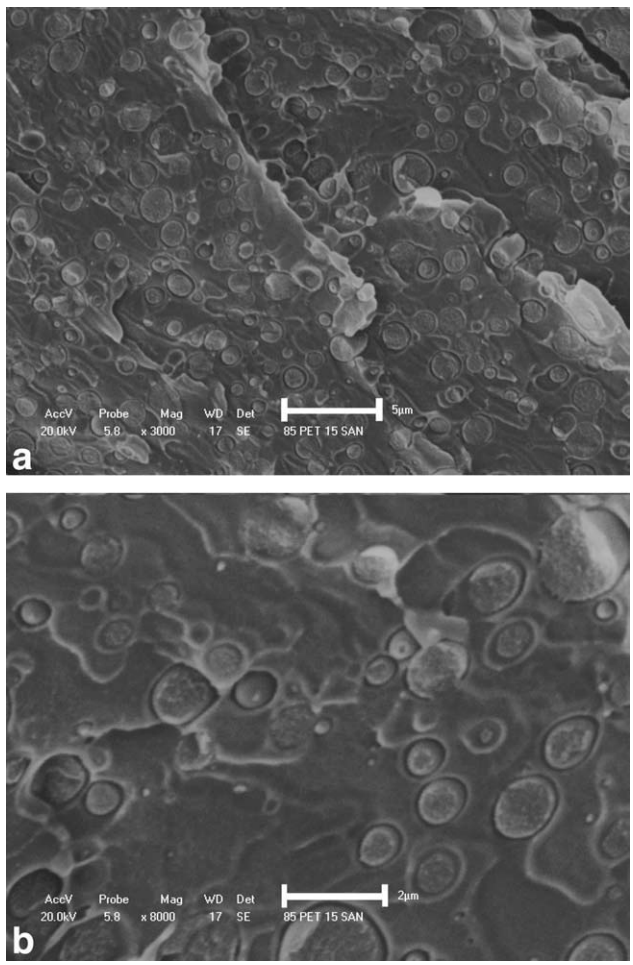

Figure 11 SEM images of a PET/SAN blend with 15% SAN (a) and PET/PS blend with 15% PS (b).

Equilibrium melting temperature and crystallinity

A study of the melting behavior was conducted with DSC for PET and PET/SAN blend previously subjected to isothermal cold crystallization; selected melting endotherms are given in Figure 10.

Combining the isothermal cold crystallization temperatures with the melting endotherms, the equilibrium melting temperature (T_m^0) of neat PET and the PET/SAN blend was calculated using Hofmann–Weeks method;[9] the values are summarized in Table IV. The equilibrium melting temperature of pure PET, $T_m^0 \approx 255$°C is well within the interval (245°C to 265°C) quoted in the literature.[62,68–72] The presence of 1% SAN resulted in a small but significant (about 7°C) reduction of the melting point of PET.

Total crystallinity was not affected by the addition of 1% SAN. However, the rate of crystallization was very much affected by the small addition of SAN, as discussed before: average crystallization rate for the blend was between 1/5 to slightly over 1/2 of the rate of crystallization of the neat PET. This behavior may indicate a disturbance of the crystallization process by the noncrystallizable polymer.

TABLE V
Effect of Crystallinity and 1% SAN Addition on the Tensile Properties of PET

State	Composition	Young's modulus (MPa)	Yield stress (MPa)	Elongation at break (%)
Amorphous	PET	1701 ± 42	46.9 ± 0.7	245 ± 7
	PET/SAN (1%)	1688 ± 40	46.8 ± 0.9	243 ± 7
Semicrystalline	PET	1913 ± 48	70.1 ± 1.4	5.7 ± 0.2
	PET/SAN (1%)	2054 ± 51	69.5 ± 1.0	5.9 ± 0.2

Observation of SEM

The morphology of a PET/SAN blend with 15% SAN was examined by scanning SEM on cold fractured amorphous samples. Example image is shown in Figure 11(a), along with a similar microphotography of a PET/PS blend with 15% PS in the same scale, Figure 11(b). A two-phase structure composed by a PET matrix and nearly spherical particles of SAN and PS can be clearly noticed. Most SAN particles remained attached to the matrix on the fractured surface, which may indicate some measure of PET/SAN interfacial interactions. SAN is a polar copolymer, capable of "chemical" (dipole–dipole) interactions, which may be responsible for a significant adhesion of the spherical particles to the PET matrix. In the PET/PS blend, as PS is apolar, "chemical" interactions are less intense and the phases remain mobile, as verified elsewhere.[4,10]

The average diameter of the dispersed domains of SAN and PS were 1.2 and 2.4 μm, respectively, calculated from eq. (2). According to Favis and Willis,[73] blends with mobile interfaces (immiscible blends) coalesce very easily and the domain size is highly dependent on composition. Compared with the PET/PS blend, the stronger interactions in the PET/SAN blend contributes to greater adherence between the phases and to the formation of smaller particles.

Mechanical properties

Tensile properties of PET and its blend with 1% SAN are shown in Table V, for amorphous and semicrystalline samples. Higher values of Young's modulus and yield stress are observed for crystallized PET, which also shows a dramatic drop in the elongation at break. These effects may be attributed to restrictions molecular mobility. Results agree with those reported in the literature.[74] Table V also shows that the addition of SAN does not affect the mechanical properties of PET. This observation is important for the applications: it shows that the reduction in the rate of cold crystallization of PET by the presence of 1% SAN does not compromise the mechanical behavior of the material.

CONCLUSIONS

The isothermal cold crystallization of PET and PET/SAN blends was analyzed in detail. SEM microphotographs show that PET/SAN blends form predominantly a two-phase mixture. However, the variation in glass transition temperature suggests a limited solubility among the polymers. The presence of only 1% SAN retarded significantly the cold crystallization rate, reflected also by the Avrami parameters and suggesting that SAN is acting as an antinucleating additive for PET. Results show that the addition of only 1% of SAN extends the operating window for blow molding processing, without changing product properties or manufacturing procedures.

The authors acknowledge Rhodia-Ster (now M&G) for PET; RMRW is grateful to CAPES (Brazil), for a research fellowship.

References

1. Mandelkern, L. Crystallization of Polymers. 2: Kinetics and Mechanisms; Cambridge University Press: Cambridge, 2004.
2. Olabisi, O.; Robeson, L. M.; Shaw, M. T. Polymer-Polymer Miscibility; Academic Press: New York, 1979.
3. Utracki, L. A. Polymer Blends Handbook; Kluwer Academic Publishers: Dordrecht, 2002.
4. Wellen, R. M. R.; Rabello, M. S. J Appl Polym Sci 2009, 114, 1884.
5. Wellen, R. M. R.; Rabello, M. S. J Appl Polym Sci 2010, 116, 1077.
6. Avrami, M. J Chem Phys 1939, 7, 1103.
7. Avrami, M. J Chem Phys 1940, 8, 212.
8. Avrami, M. J Chem Phys 1941, 9, 177.
9. Hoffman, J. D.; Weeks, J. J. J Res Natl Bur Stand Sect A Phys Chem 1962, 66A, 13.
10. Wellen, R. M. R. Ph.D. Thesis, Universidade Federal de Campina Grande, Brasil, 2007.
11. Ballara, A.; Verdu, J. Polym Degrad Stab 1989, 26, 361.
12. Supaphol, P.; Apiwanthanakorn, N. J Polym Sci Part B: Polym Phys 2004, 42, 4151.
13. Allen, N. S.; Edge, M.; Mohammadian, M. Eur Polym J 1991, 27, 1373.
14. Seo, K. S.; Cloyd, J. D. J Appl Polym Sci 1991, 42, 845.
15. Karagiannidis, P. G.; Stergiou, A. C.; Karayannidis, G. P. Eur Polym J 2008, 44, 1475.
16. Roberts, R. C. Polymer 1969, 10, 113.
17. Starkweather, H. W., Jr.; Zoller, P.; Jones, G. A. J Polym Sci Polym Phys Ed 1983, 21, 295.
18. Canevarolo, S. V., Jr. Técnicas de Caracterização de Polímeros; Artliber: São Paulo, 2004.

19. Jose, S.; Thomas, S.; Biju, P. K.; Koshy, P.; Karger-Kocsis, J. Polym Degrad Stab 2008, 93, 1176.
20. Maa, C. T.; Chang, F. C. J Appl Polym Sci 1993, 49, 913.
21. Akiyama, M.; Jamieson, A. M. Polymer 1992, 33, 3582.
22. Oyama, H. T.; Kitagawa, T.; Ougizawa, T.; Inoue, T.; Weber, M. Polymer 2004, 45, 1033.
23. Wellen, R. M. R.; Rabello, M. S. J Mater Sci 2005, 40, 6099.
24. Pingping, Z.; Dezhu, M. Eur Polym J 1999, 33, 1817.
25. Lu, X. F.; Hay, J. N. Polymer 2001, 42, 9423.
26. Kint, D. P. R.; Rudé, E.; Llorens, J.; Muñoz-Guerra, S. Polymer 2002, 43, 7529.
27. Banks, W.; Gordon, M.; Roe, R. J.; Sharples, A. Polymer 1963, 4, 61.
28. Mandelkern, L. Crystallization of Polymers; McGraw-Hill: New York, 1964.
29. Wellen, R. M. R.; Rabello, M. S. Polímeros: Ciências e tecnologia 2007, XVII, 113.
30. Reinsch, V. E.; Rebenfeld, L. J Appl Polym Sci 1996, 59, 1913.
31. Schultz, J. M. Polymer Materials Science; Prentice-Hall: New Jersey, 1974.
32. Jabarin, S. A. J Appl Polym Sci 1987, 34, 97.
33. Groeninckx, G.; Berghmans, H.; Overbergh, N.; Smets, G. J Polym Sci Polym Phys Ed 1974, 12, 303.
34. Jabarin, S. A. J Appl Polym Sci 1987, 34, 85.
35. Skoglund, P.; Fransson, A. J Appl Polym Sci 1996, 61, 2455.
36. Bose, S.; Bhattacharyya, A. R.; Kodgire, P. V.; Misra, A.; Pötschke, P. J Appl Polym Sci 2008, 106, 3394.
37. Cheng, H.; Tian, M.; Zhang, L. J Appl Polym Sci 2008, 109, 2795.
38. Keith, H. D.; Padden, F. J., Jr. J Appl Phys 1964, 35, 1270.
39. Keith, H. D.; Padden, F. J., Jr J Appl Phys 1964, 35, 1286.
40. Martuscelli, E.; Silvestre, C.; Bianchi, L. Polymer 1983, 24, 1458.
41. Dreezen, G.; Koch, M. H. J.; Reynaers, H.; Groeninckx, G. Polymer 1999, 40, 6451.
42. Di Lorenzo, M. L. Prog Polym Sci 2003, 28, 663.
43. Martuscelli, E.; Silvestre, C.; Abate, G. Polymer 1982, 23, 229.
44. Cheng, S.; Shanks, R. J Appl Polym Sci 1993, 47, 2149.
45. Run, M.; Wu, S.; Zhang, D.; Wu, G. Polymer 2005, 46, 5308.
46. Molinuevo, C. H.; Mendez, G. A.; Müller, A. I. J Appl Polym Sci 1998, 70, 1725.
47. Gao, G.; Zhang, L.; Sun, H.; Chen, G.; Zhang, M.; Ma, R.; Liu, F. J Appl Polym Sci 2005, 97, 878.
48. Xiao, J.; Zhang, H.; Wan, X.; Zhang, D.; Zhou, Q.; Woo, E. M.; Turner, S. R. Polymer 2002, 43, 3683.
49. Li, B.; Yu, J.; Lee, S.; Ree, M. Polymer 1999, 40, 5371.
50. Yoshikai, K.; Nakayama, K.; Kyotani, M. J Appl Polym Sci 1996, 62, 1331.
51. Bian, J.; Ye, S. R.; Feng, L. X. J Polym Sci Part B: Polym Phys 2003, 41, 2135.
52. Yoshihara, N.; Shibaya, M.; Ishihara, H. J Polym Eng 2005, 25, 97.
53. Connor, D. M.; Allen, S. D.; Collard, D. M.; Liotta, C. L.; Schiraldi, D. A. J Appl Polym Sci 2001, 80, 2696.
54. Kang, H.; Lin, Q.; Armentrout, R. S.; Long, T. E. Macromolecules 2002, 35, 8738.
55. Lorenzo, A. T.; Arnal, M. L.; Albuerne, J.; Müller, A. J. Polym Test 2007, 26, 222.
56. Piorkowska, E.; Galeski, A.; Haudin, J. M. Prog Polym Sci 2006, 31, 549.
57. Avila-Orta, C. A. A.; Rodríguez, F. J. M.; Wang, Z. G.; Rodrígues, D. N.; Hsiao, B. S.; Yeh, F. Polymer 2003, 44, 1527.
58. Calvert, P. D.; Ryan, T. G. Polymer 1984, 25, 921.
59. Caminiti, R.; D'Ilario, L.; Martinelli, A.; Piozzi, A. Macromol Chem Phys 2001, 202, 2902.
60. Dreezen, G.; Fang, Z.; Groeninckx, G. Polymer 1999, 40, 5907.
61. Jonas, A.; Legras, R. Polymer 1991, 32, 2691.
62. Hwang, J. C.; Chen, C. C.; Chen, H. L.; Yang, W. C. O. Polymer 1997, 38, 4097.
63. Morgan, R. L.; Hill, M. J.; Barham, P. J. Polymer 1999, 40, 337.
64. Wang, C.; Lin, C. C.; Tseng, L. C. Polymer 2006, 47, 390.
65. Li, W.; Kong, X.; Zhou, E.; Ma, D. Polymer 2005, 46, 11655.
66. Cebe, P.; Hong, S. Polymer 1986, 27, 1183.
67. Liu, S.; Yu, Y.; Cui, Y.; Zhang, H.; Mo, Z. J Appl Polym Sci 1998, 70, 2371.
68. Van Antwerpen, F.; Van Krevelen, D. W. J Polym Sci Polym Phys Ed 1972, 10, 2435.
69. Fakirov, S.; Fischer, E. W.; Hoffmann, R.; Schimidt, G. F. Polymer 1977, 18, 1121.
70. Groeninckx, G.; Reynaers, H.; Berghmans, H.; Smerts, G. J Polym Sci Polym Phys Ed 1980, 18, 1311.
71. Vilanova, P.; Ribas, S.; Guzman, G. Polymer 1985, 26, 423.
72. Rahman, M. H.; Nandi, A. K. Macromol Chem Phys 2002, 203, 653.
73. Favis, B. D.; Willis, J. M. J Polym Sci Part B: Polym Phys 1990, 28, 2259.
74. Torres, N.; Robin, J. J.; Boutevin, B. Eur Polym J 2000, 36, 2075.